Journal of Power Sources 215 (2012) 99–108

Contents lists available at SciVerse ScienceDirect

Journal of Power Sources

journal homepage: www.elsevier.com/locate/jpowsour

Nanocomposites of gold and poly(3-hexylthiophene) containing fullerene moieties: Synthesis, characterization and application in solar cells

Jilian N. de Freitas [a], Messai A. Mamo [b,c], Manoko Maubane [b,c], Willem A.L. van Otterlo [c,d], Neil J. Coville [b,c], Ana Flavia Nogueira [a,*]

[a] Laboratory of Nanotechnology and Solar Energy, P.O. Box 6154, Chemistry Institute, University of Campinas (UNICAMP), 13083-970 Campinas-SP, Brazil
[b] DST/NRF Centre of Excellence in Strong Materials, University of the Witwatersrand, PO Wits, 2050 Johannesburg, South Africa
[c] Molecular Sciences Institute, School of Chemistry, University of the Witwatersrand, PO Wits, 2050 Johannesburg, South Africa
[d] Department of Chemistry and Polymer Sciences, Stellenbosch University, Stellenbosch, Western Cape, South Africa

HIGHLIGHTS

► New nanocomposites based on P3HT, C_{60} and gold nanoparticles were synthesized.
► Functionalized C_{60} was covalently linked to P3HT chains.
► The presence of C_{60} affects the size and the concentration of gold nanoparticles.
► The nanocomposites were applied as sensitizers or co-sensitizers in solar cells.
► Using ternary-based nanocomposites enhanced the photocurrent of devices.

ARTICLE INFO

Article history:
Received 18 January 2012
Received in revised form
14 April 2012
Accepted 23 April 2012
Available online 28 April 2012

Keywords:
Poly(3-hexylthiophene)
Fullerene
Gold nanoparticles
Nanocomposites
Dye-sensitized solar cells
Organic solar cells

ABSTRACT

Functionalized C_{60} was reacted with 3-hexylthiophene in the presence of $FeCl_3$ to produce a copolymer (P3HT-C_{60}) containing 3-hexylthiophene units as the main chain, with C_{60} side groups. Gold nanoparticles (AuNPs) were synthesized in the presence of poly(3-hexylthiophene) (P3HT), or P3HT-C_{60} copolymer, using a two-phase, one–pot reaction involving the reduction of $HAuCl_4$ by $NaBH_4$. This approach resulted in the formation of nanocomposites where AuNPs are directly stabilized with P3HT or P3HT-C_{60}. All the materials were characterized using UV–vis absorption and fluorescence spectroscopy, X-ray diffraction and high-resolution transmission electron microscopy, and were applied as sensitizers or co-sensitizers in dye-sensitized solar cells. The synergistic effect in the ternary component nanocomposite introduced by the presence of C_{60} and AuNPs resulted in devices with higher photocurrents compared to standard devices.

1. Introduction

The use of electron-accepting fullerenes, in combination with π-conjugated systems as electron donors, offers several attractive features. In particular, fullerene accelerates charge separation and decelerates charge recombination, compared to two-dimensional, planar electron acceptors [1]. This is beneficial for stabilizing the charge-separated state in C_{60}-based materials, as required in artificial electron transfer systems [2,3].

In solar cells, conjugated polymers containing thiophene rings, such as poly(3-hexylthiophene) (P3HT), play a crucial role as electron donors and in charge transport [4–6]. The design of conjugated polymers covalently linked to C_{60} has thus received increasing attention in the past few years due to their potential for photoelectronic applications [7–18]. These systems have been designed to achieve efficient intramolecular energy/charge transfer. In addition, the particular problem of phase segregation in bi-component composite materials used in such devices is thought to be minimized.

The addition of metal nanoparticles to solar cells is also an elegant way to improve the efficiency of these devices, through exploration of the plasmon resonance effect. In organic solar cells (OSC), the incorporation of metal nanoparticles, such as gold, as buffer layers is perhaps the most used approach [19–23]. However, advantage may also be taken from the incorporation of these

* Corresponding author. Tel.: +55 19 35213029; fax: + 55 19 35213023.
E-mail address: anaflavia@iqm.unicam.br (A.F. Nogueira).

0378-7753 © 2012 Elsevier B.V. Open access under the Elsevier OA license.
doi:10.1016/j.jpowsour.2012.04.066

nanoparticles into the bulk heterojunction [24–27]. In this case, gold nanoparticles (AuNPs) may be used in combination with P3HT and/or PCBM ([6,6]-phenyl-C_{61}-butyric acid methyl ester). Nanoparticles have increased the photoluminescence when combined with P3HT. This was explained by polymer chain separation induced by the presence of the nanoparticles [28]. P3HT can also bind to Au, leading to direct electron transfer from the polymer to the nanoparticles. Electron transfer from metal to C_{60} has also been reported [29–31].

In most cases, polymer, AuNPs and fullerene are typically mixed together by depositing a co-solution of all materials. Interestingly, only a few papers have systematically investigated morphological changes introduced by the presence of metal nanoparticles in the films. In an earlier work, Conturbia [32] has shown that, in fact, the morphology of the P3HT system is significantly changed upon incorporation of AuNPs. The results suggested that the morphologic changes induced by incorporation of Au may act in the way of organization/crystallization of PCBM and/or P3HT, and that this parameter is responsible for improving or decreasing device efficiency [33].

In dye-sensitized solar cells (DSSCs), P3HT has been used as sensitizer and/or as hole conductor, in combination with a TiO_2 nanoporous electrode [34–39], while AuNPs have been shown to cause an increase in the photocurrent related to the plasmon effect contribution to light absorption/charge separation [40–42]. C_{60} and its derivatives can also be incorporated into DSSCs: C_{60} clusters can act as electron shuttles, which effectively regenerate the sensitizer but at the same time minimize direct interaction between the excited sensitizer and the redox couple in the electrolyte [43].

In this paper, we report a simple route to synthesize ternary component-based nanocomposites. Initially, the functionalization of C_{60} using azomethine ylides (Prato's reaction) was carried out, followed by a polymerization reaction to covalently link C_{60} to P3HT. The resulting copolymer, containing P3HT segments as main chain and C_{60} moieties as side chains, was impregnated with AuNPs, resulting in formation of a ternary component-based nanocomposite. The optical, structural and thermal properties of these nanocomposites were investigated and compared to those of a P3HT-C_{60} copolymer and pristine P3HT impregnated with AuNPs. All the materials were applied in DSSCs as sensitizers or co-sensitizers.

2. Experimental

2.1. Functionalization of C_{60}

Functionalization of C_{60} was achieved using the procedure developed by Prato and collaborators [44]. C_{60} (0.50 g, 0.69 mmol) was added to pre-dried toluene (~75 mL). The mixture was heated to 115 °C to dissolve all the C_{60} and 3-thiophenecarboxaldehyde (0.077 g, 0.69 mmol) was added to the toluene solution. *N*-methylglycine (0.13 g, 1.426 mmol) was then added to the reaction mixture in small portions over 5 days (about 25 mg per 24 h). The reaction mixture was left under reflux and continuous stirring for five days. The purple color of the solution slowly changed to brown. The solvent was removed under reduced pressure to afford a brown solid, which was purified using column chromatography (SiO_2, toluene, then 1% DMF in toluene) and dried under vacuum for 48 h to afford **f-C_{60}** (0.49 g, 83% based on C_{60}). *m/z*: 2.6%, 860 [M+1], FTIR: 2992–2720, 696, 526 cm^{-1}. CHN: C_{60} (C 99.32%, H 0.05%, N 0.11%); f-C_{60} (C 90.59%, H 1.67%, N 1.76%).

2.2. Synthesis of P3HT

Synthesis of P3HT was obtained by a simple route, using $FeCl_3$ as catalyst [45]. $FeCl_3$ (2.0 g) was added to dry chloroform (~12 mL) and stirred for 10 min. 3-hexylthiophene (0.50 g, 3 mmol) in dry chloroform (~12 mL) was then added drop-wise and the reaction mixture was stirred overnight under Ar. The polymerization reaction was terminated by pouring the reaction mixture into excess methanol (~30 mL). The crude polymer precipitate was filtered using a PTFE membrane filter (1 μm, Millipore) and washed with ethanol, 1:1 v/v distilled water:acetone mixture, and finally with acetone. The dark brown solid product was dried under vacuum for 48 h to afford **P3HT** (0.45 g, 90%).

2.3. Synthesis of P3HT-C_{60} copolymer

The synthesis of P3HT-C_{60} copolymer was performed according to the method reported by Mamo et al. [46,47]. $FeCl_3$ (2.0 g) was added to dry dichloromethane (~25 mL) and stirred under argon for about 15 min. A mixture of 3-hexylthiophene (0.5 g, 2.97 mmol) and **f-C_{60}** (5.1 mg, 0.0059 mmol) in the molar ratio 500:1 was dissolved in dry dichloromethane (~10 mL) and added to the $FeCl_3$ mixture drop-wise over 25 min. The reaction mixture was stirred overnight. Methanol (~50 mL) was added and the precipitate was filtered using a PTFE membrane filter (1 μm, Millipore) and washed with ethanol, 1:1 (v/v) distilled water:acetone mixture, and finally with acetone. The brown solid was dried under reduced pressure for 48 h to afford **P3HT-C_{60}** (0.28 g, 57% based on 3-hexylthiophene).

2.4. Synthesis of P3HT- and P3HT-C_{60}-capped AuNPs

Synthesis of P3HT-capped AuNPs and P3HT-C_{60}-capped AuNPs (P3HT-C_{60}-Au nanocomposite) were achieved using an adaptation of the procedure reported by Zhai and McCullough [48]. Tetraoctylammonium bromide (0.27 g, 0.5 mmol) was added to 8 mL of toluene in a 25 mL round bottom flask and stirred until dissolved. Then, an aqueous solution of $HAuCl_4$ (3 mL, 0.1 mmol) was added and the two-phase mixture was stirred vigorously until all the tetrachloroaurate was transferred into the organic layer. This was determined by observing a color change of the aqueous phase from yellow to colorless. P3HT or P3HT-C_{60} (15 mg) was dissolved in 3 mL of toluene and added to the mixture. The mixture was stirred for 3 h. A freshly prepared aqueous solution of sodium borohydride (2.5 mL, 10 mmol) was added slowly to the mixture with vigorous stirring. The mixture was stirred overnight before quenching in methanol. Purification was obtained by filtering the resulting mixture with a PTFE membrane filter (0.45 μm, Millipore) and washing with methanol and water, to afford **P3HT-Au** or **P3HT-C_{60}-Au** nanocomposites.

2.5. Material characterizations

The optical characteristics of chloroform solutions (1 mg mL^{-1}) of P3HT, P3HT-C_{60}, P3HT-Au and P3HT-C_{60}-Au were obtained. UV–vis spectra were recorded on a Hewlett–Packard 8453 diode array spectrophotometer and fluorescence spectra were measured with an ISS PC1TM Photon Counting Spectrofluorometer, operating at room temperature (excitation = 430 nm). Powder X-ray diffraction (XRD) data were obtained using a Shimadzu XRD 7000 diffractometer with CuKα, 40 kV, 30 mA and 2° min^{-1} scanning rate, over the range 2–80°. Thermogravimetric analysis (TGA) was performed using a Thermogravimetric Analyser 2950 from TA Instruments. All measurements were done under a continuous argon flow of 100 mL min^{-1}, heating from room temperature to 900 °C at a heating rate of 10 °C min^{-1}. High-resolution transmission electron microscopy (HRTEM) images were acquired in an HRTEM-JEM 3010 URP operating at 300 kV with resolution of 0.17 nm. The samples were prepared by casting one drop of

a dispersion of materials in chloroform onto a copper grid (300 mesh) pre-covered with a thin holey carbon layer. Molar mass determinations were made by gel permeation chromatography (GPC) at a flow rate of 1 mL min^{-1} in chloroform on a Shimadzu Class-LC10 HPLC equipped with three Supelco Progel columns (G5000 + G4000 + G3000). The molar mass is reported relative to narrow dispersity polystyrene standards (2500, 5000, 17 500, 30 000, 50 000, 95 800 and 184 200). Only the fraction of the material that was fully dispersed in chloroform and could be filtered though a PTFE membrane filter (0.45 μm, Millipore) was analyzed using this technique.

2.6. Solar cell assembly

A typical assembly procedure for a "standard" DSSC device was carried out as follows: a TiO_2 nanoporous film was prepared by spreading a small aliquot of a commercial colloidal suspension (Ti-Nanoxide T, Solaronix) onto an FTO (fluorine doped tin oxide) glass substrate (Hartford Glass Co., 8–12Ω). The film was heated to 450 °C for 30 min, generating a layer of ~4 μm thickness as measured with a Taylor Hobson precision Formtalysurf 50. The electrodes were immersed in a 1×10^{-4} mol L^{-1} solution of the sensitizer *cis*-diisothiocyanato-bis(2,2′-bipyridyl-4,4′-dicarboxylato)ruthenium(II) bis(tetrabutylammonium)(N719, Solaronix) in ethanol for 20 h at room temperature. Afterwards, the electrodes were washed with ethanol and dried in air. The liquid electrolyte was prepared from LiI (0.10 mol L^{-1}), I_2 (0.05 mol L^{-1}), tetrabutylammonium iodide (0.80 mol L^{-1}) and 4-tertbutylpyridine (0.50 mol L^{-1}) in an acetonitrile:3-methoxypropionitrile (1:1 (v/v)) mixture. The counter-electrode consisted of a Pt film deposited by sputtering on top of an FTO-glass substrate.

Devices using the materials synthesized in this work were obtained by a similar assembly procedure. First, P3HT, P3HT-C_{60}, P3HT-Au or P3HT-C_{60}-Au were used as sensitizers (in substitution of the N719 dye) by casting 20 μL of a 1 mg mL^{-1} toluene solution of the materials on top of the TiO_2 film, prior to electrolyte deposition. Alternatively, these materials were used as co-sensitizers in the devices. In this case, 20 μL of a 1 mg mL^{-1} toluene solution of the materials were deposited on top of the TiO_2 film previously sensitized with N719 dye. All the devices were assembled with 0.15 cm^2 of active area.

J–*V* curves were obtained under standard AM 1.5 conditions using a 150 W Xe lamp as light source and appropriate filters. The polychromatic light intensity (100 mW cm^{-2}) at the electrode position was measured with a silicon photodiode from Newport Optical Power Meter, model 1830-C.

3. Results and discussion

3.1. Material properties

Scheme 1 shows the synthetic route used to obtain nanocomposites based on P3HT, C_{60} and AuNPs. Initially, functionalization of C_{60} was carried out via the Prato reaction: 3-thiophenecarboxyaldehyde and *N*-methylglycine react to form azomethine ylides at high temperatures, which react via a 1,3-dipolar cycloaddtion with C_{60}. Functionalized C_{60} (**f-C_{60}**) was then reacted with 3-hexylthiophene using $FeCl_3$ as catalyst, resulting in a copolymer containing poly(3-hexylthiophene) as the main chain, with C_{60} moieties as side groups (**P3HT-C_{60}**).

One advantage of this method is that C_{60} is functionalized and separated from un-reacted C_{60} before the polymerization step. Other authors have successfully used the Prato reaction to synthesize copolymers containing P3HT main-chains with methyfulleropyrrolidine as end groups [12]. In that case, the *in situ* generation of the macromolecular azomethine ylide intermediate induced the coupling of the polymer chains, which increased the molar mass and polydispersivity measured with GPC against polystyrene standards, but lowered the content of C_{60} loaded into the sample [12]. In this work, the 3-hexylthiophene:C_{60} ratio used in the polymerization was 500:1. Larger amounts of C_{60} were found to result in polymers with low solubility in common organic solvents. A common approach used to enhance the solubility in C_{60}-containing materials is the synthesis of rod-coil triblock copolymers, where a coil block made of polystyrene, for example, is placed between the P3HT and the C_{60}-containing blocks to increase the solubility of the copolymer and to act as a spacer [11]. The non-conjugated spacer block reduces the chance of interchain recombination of free holes and electrons, but, at the same time, it can damage the charge carrier transport since it is mainly composed of insulating moieties. In this work, as we aim at applications in excitonic solar cells, charge transport is a key parameter.

In parallel, poly(3-hexylthiophene) stabilized gold nanoparticles (**P3HT-Au**) were synthesized using the method reported by Zhai and McCullough [48]. This consisted of a room temperature, two-phase, one–pot reaction involving the reduction of $HAuCl_4$ by $NaBH_4$ in the presence of the polymer. In composites synthesized this way, the gold nanoparticles are stabilized by the interaction of the sulfur atoms of the polymer with the gold surface. In this paper, a new ternary component-based nanocomposite (**P3HT–C_{60}-Au**), obtained by capping AuNPs with P3HT-C_{60} copolymer, was prepared (Scheme 1).

From thermogravimetric analysis it was observed that all the materials have thermal stability up to 300 °C under inert atmospheres, which is adequate for application in solar cells. The concentration of C_{60} in the copolymer was estimated to be ~ 2 ± 1 wt%, as calculated by the difference from the residues obtained at 600 °C from the degradation curves of P3HT and P3HT-C_{60} samples. This value is higher than expected based on the molar ratio between 3-hexylthiophene and C_{60} added to the reaction medium (500:1). Considering the reaction yield (~57%), we can infer that a significant fraction of the monomer did not react, resulting in polymer segments with small chains containing larger amounts of C_{60} moieties.

GPC analysis was carried out to estimate the molar masses (Mw) of these materials. It was found that the Mw is 2585 g mol^{-1} and 820 g mol^{-1} for P3HT and P3HT-C_{60}, respectively, indicating that the samples may be mainly composed of small chains. Besides, it seems that the presence of f-C_{60} in the reaction medium leads to the formation of a polymer with lower molar mass, compared to pristine P3HT synthesized via the same route. However, GPC results must be interpreted carefully for two reasons: (i) the exclusion volume of C_{60} is greater than an equivalent molar mass polystyrene standard; (ii) only the fraction of the material that could be dispersed in chloroform and filtered was analyzed (*i.e.*, the fraction of the material with smaller chains and/or less concentration of C_{60} in the chain). The molar masses recently reported by other authors for conjugated polymers covalently linked to C_{60} are in the range 5000 g mol^{-1} to 20000 g mol^{-1} [7,12,14,15,49]. These values are higher than the ones reported here, but this comparison is not straightforward, since most of the materials have different main chain chemical structures.

For the thermogravimetric analysis of P3HT-Au and P3HT-C_{60}-Au samples, the residue at temperatures higher than 750 °C is expected to be composed mostly of gold. From the difference between the residue contents of these samples to those of P3HT and P3HT-C_{60}, one can estimate the amount of gold loaded into the composites as being ~ 25 wt% for P3HT-Au and ~ 35 wt% for P3HT-C_{60}-Au. The larger AuNPs uptake in the ternary composite suggests that, during the synthesis the interaction between P3HT-C_{60} with AuNPs is different from that of bare P3HT with AuNPs. Possibly, the presence

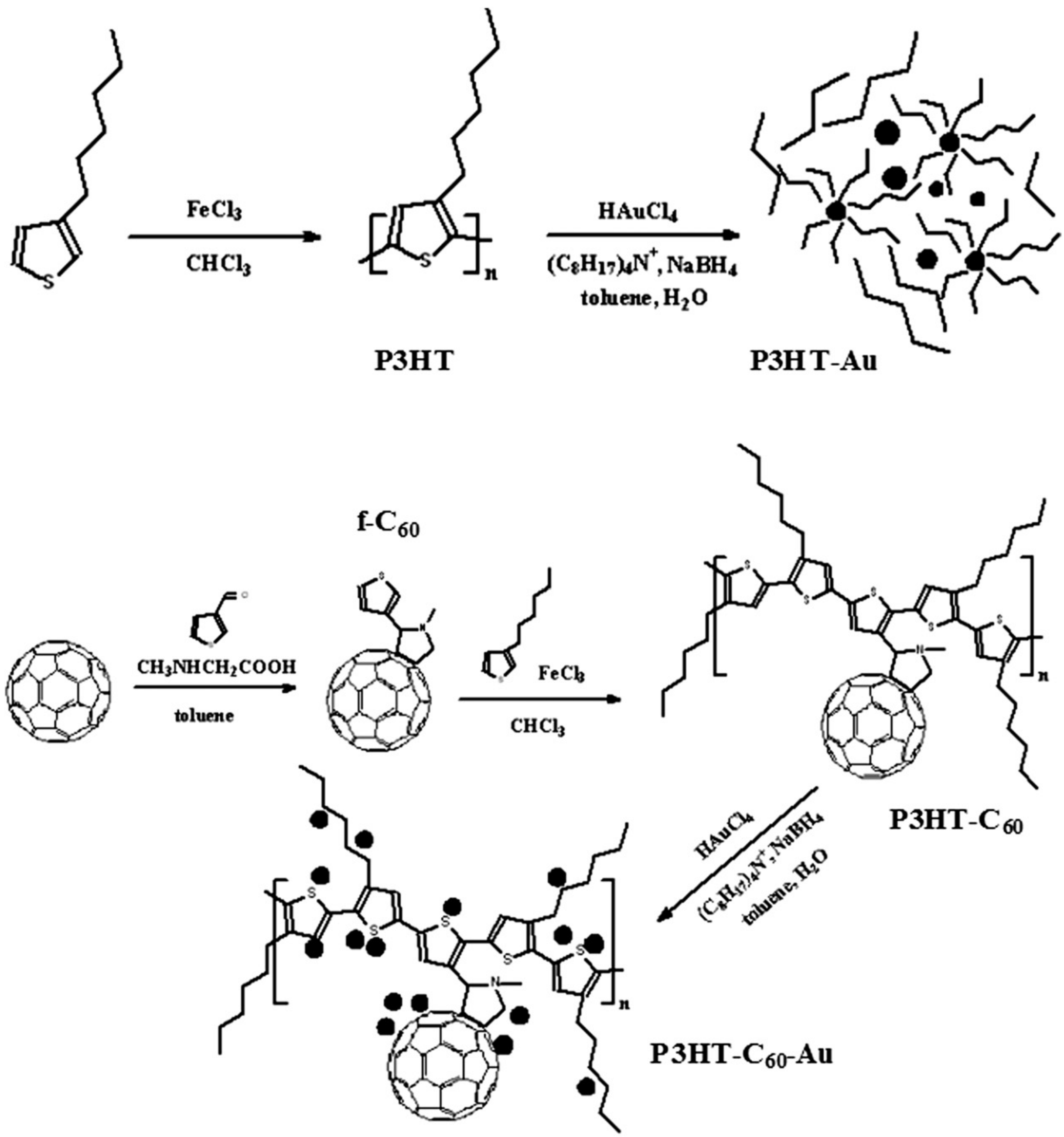

Scheme 1. Synthesis of polymer, copolymer and nanocomposites based on P3HT, C_{60} and AuNPs. Black spots represent AuNPs and lines represent polymeric chains.

of C_{60} side groups in the copolymer induces steric effects in the local polymer chain region, leaving more thiophene segments “free” to interact with the nanoparticles, resulting in the uptake of a larger number of AuNPs. Also, the presence of C_{60} may change the diffusion rate of the polymeric chains in the reaction medium.

Fig. 1 shows the normalized absorption and emission spectra of all the synthesized materials in chloroform solution. The main absorption band observed at 430 nm in the UV–vis spectrum of P3HT and P3HT-Au samples is attributed to the $\pi-\pi^*$ transition of the conjugated polymer chain [50]. Unlike previous reports [48,51], we did not observe the gold surface plasmon resonance signal at ~530 nm in the absorption spectra of the P3HT-Au solution. The lack of this signal may be due to spectral overlap between the plasmons and the polymer.

P3HT-C_{60} copolymer and P3HT-C_{60}-Au nanocomposite show a red-shift in the absorption maxima to 442 nm. In principle, this shift could be indicative of a higher organization (stacking) of P3HT chains, or due to a change in the polymer conformation. Since the photoluminescence spectra of these samples is not broadened in comparison to that of P3HT, the formation of aggregates is not suggested. In the emission spectra, increased formation of aggregates is only seen for the P3HT-Au material (Fig. 1b).

Another characteristic of the P3HT-C_{60} copolymer and the P3HT-C_{60}-Au nanocomposite is that, despite the strong extinction coefficient of fullerenes, only a discrete shoulder at 330–340 nm attributed to the absorption by this molecule was observed. Other authors have observed a more prominent peak for the absorption of C_{60} in copolymers containing this molecule [7,11,12]. This is possibly

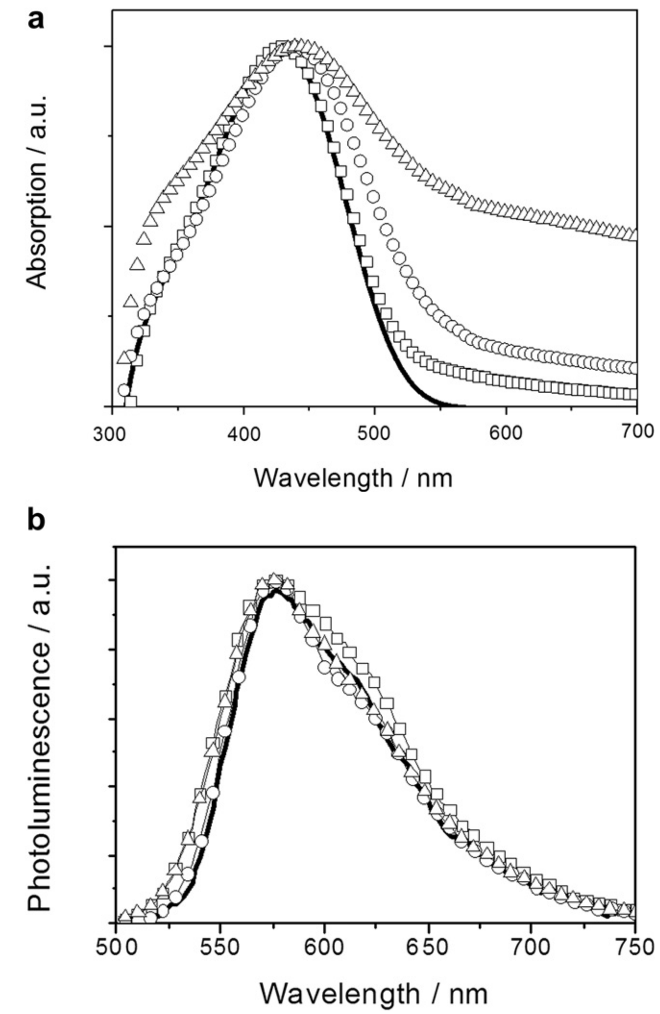

Fig. 1. Normalized (a) absorption and (b) photoluminescence spectra of 1 mg mL^{-1} chloroform solution of (▬) P3HT, (-□-) P3HT-Au, (-○-) P3HT-C_{60} and (-Δ-) P3HT-C_{60}-Au.

related to a higher content of C_{60} in those samples, compared to this work.

The P3HT-C_{60}-Au nanocomposite shows a broader absorption in the wavelength region from 500 to 700 nm, and this could be indicative of long-range order of the polymer chains caused by self-assembly of the polymer on the nanoparticles [52], or it can be related to the plasmon peak of AuNPs. Interestingly, the comparison of the absorption and photoluminescence spectra of P3HT-Au and P3HT-C_{60}-Au nanocomposites reveals that these samples have different optical features. Probably these differences result from the plasmon resonance effect, which can be observed in the ternary composite spectra, due to a larger concentration of AuNPs in this sample. This results in a red-shift in the plasmon absorption wavelength (because the AuNPs are closer to each other in this sample), which in turn would decrease the spectral overlap with P3HT, leading to the broad absorption spectra seen in Fig. 1a.

Table 1 summarizes the maximum absorption and emission wavelengths observed for all the materials investigated. Our findings reveal that the optical characteristics of all the materials are dominated by the characteristics of P3HT, consistent with the findings of other authors for physical mixtures of P3HT, PCBM and AuNPs [25,26,32].

The presence of C_{60} and AuNPs in the materials was observed by XRD analysis. Fig. 2 shows the X-ray diffractograms of pristine C_{60},

Table 1
Optical characterization of synthesized polymeric materials: maximum absorption wavelength ($\lambda_{max,Abs}$) and maximum emission wavelength ($\lambda_{max,Em}$).

Material	$\lambda_{max,Abs}$/(nm)	$\lambda_{max,Em}$/(nm)
P3HT	430	577
P3HT-Au	430	576
P3HT-C_{60}	440	576
P3HT-C_{60}-Au	442	576

pristine P3HT, the copolymer P3HT-C_{60} and nanocomposites P3HT-Au and P3HT-C_{60}-Au.

Crystalline C_{60} powder has the diffraction pattern displayed in Fig. 2a, where the reflections of planes (111), (220), (311), (222), (331), (420), (422) and (511) can be seen (JCPDS 44-0558), corresponding to peaks at 10.82°, 17.66°, 20.76°, 21.72°, 27.42°, 28.14°, 30.88° and 32.82°, respectively.

Pristine P3HT film has a peak at 5.20°, attributed to an interchain lamella peak with *d*-spacing ~17 Å and a peak which merges with the halo-amorphous region at 24.10° (*d*-spacing ~3.8 Å). These peaks are possibly related to crystalline orientations of the thiophene units with respect to the substrate [53,54].

For P3HT-C_{60}, the peaks attributed to polymer crystallites can still be seen, suggesting that the ordering of polymer chains is

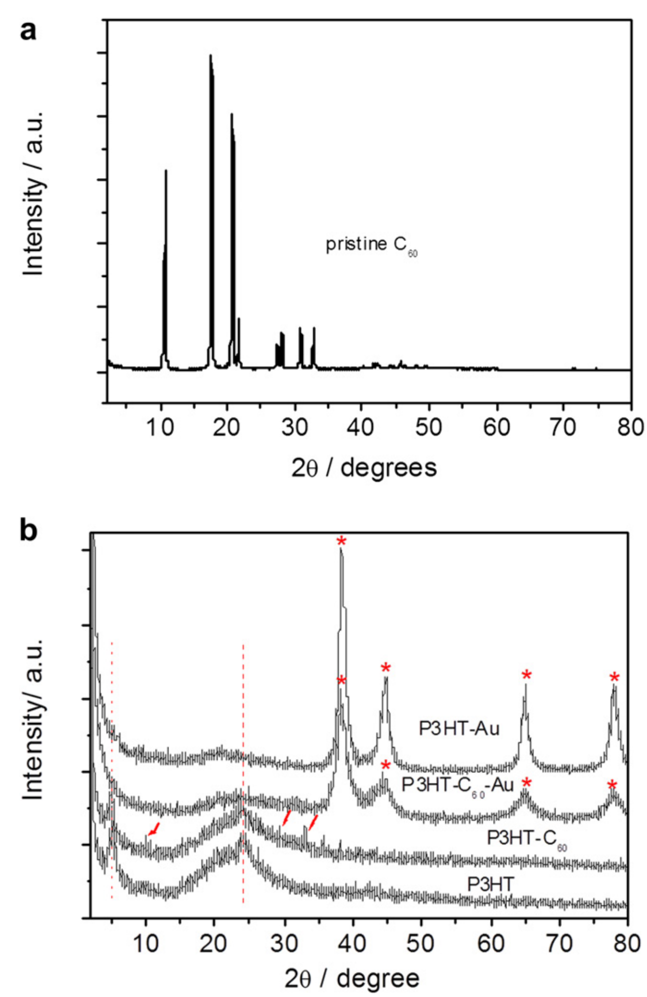

Fig. 2. XRD analysis of C_{60} (powder) and films of P3HT, P3HT-Au, P3HT-C_{60} and P3HT-C_{60}-Au. In plot (b) the lines indicate the P3HT peaks, the arrows indicate C_{60} peaks and * indicates AuNP peaks.

preserved in this material. The size of the P3HT crystallite lamella, an important parameter for charge transport, is little affected by the inclusion of the relatively bulky C_{60} groups. In addition, the fullerene units on the polymer chain do not seem to aggregate into domains with a crystal packing similar to that observed for pristine C_{60} powder, as most of the peaks attributed to C_{60} are not observed in the copolymer diffractogram. The observed features may be related to the low content of C_{60} in this copolymer.

For nanocomposites P3HT-Au and P3HT-C_{60}-Au, the reflections of the AuNPs are easily identified. The peaks at 38.42°, 44.56°, 64.82° and 77.73 corresponding to face-centered cubic (*fcc*) bulk gold patterns (111), (200), (220) and (311), respectively, (JCPDS 04-0784) indicate the crystalline structure of AuNPs loaded into the nanocomposites. Also, it seems that the presence of AuNPs disrupts the crystalline phase of the polymer. These results are different to those reported by other authors for films based on mixtures of P3HT, PCBM and AuNPs. Topp et al. [26] observed no disruption in the crystalline order of P3HT even after addition of 16 wt% of Au. Actually, for a P3HT/PCBM/Au film, Conturbia [32] observed, using atomic force microscopy, the presence of fibrillar structures and highly ordered regions. The anisotropy was more evident after addition of AuNPs, suggesting that the sample was richer in P3HT crystallites after incorporation of the metal nanoparticles [54]. Possibly the interaction between polymer and AuNPs in our composites is stronger than in films prepared by simple mixtures of the isolated components, resulting in loss of polymer crystallinity. Besides, significant phase segregation is not expected in our nanocomposites, due to the strong interaction between the S-containing polymer and the AuNPs surface.

The preferential diameter of the AuNPs was estimated to be 7.0 nm for P3HT-Au sample and 5.3 nm for P3HT-C_{60}-Au sample, using the Scherrer's equation [55] for the peak (111). This difference is related to the different structures of the polymers P3HT and P3HT-C_{60}. In P3HT, the thiophene units are less accessible to interact with growing Au nuclei. In P3HT-C_{60} copolymer, the polymeric chains uncoil due to steric effect induced by C_{60}, leaving more thiophene units "free" to interact with the AuNPs. As a result of this more effective passivation, the nanoparticles growth less (the preferential diameter of these nanoparticles is smaller). Zhai and McCullough [48] reported that the concentration of P3HT added to the reaction medium influenced the nanoparticle size and size distribution. In both of our samples the amount of P3HT added was roughly the same, thus the differences concerning AuNPs characteristics in the nanocomposites must arise from the presence of C_{60} in the reaction medium, which changes the polymer diffusion rate and swelling behavior.

The formation of AuNPs was also confirmed by HRTEM, as shown in Fig. 3. The HRTEM images of P3HT-Au and P3HT-C_{60}-Au nanocomposites show that both samples have a broad size distribution, with particles diameters varying from 1.9 nm to 12.5 nm.

3.2. Application in solar cells

Fig. 4 c shows the *J*–*V* characteristics of DSSCs assembled using the nanocomposites as sensitizers (deposition by casting of 20 μL of a 1 mg mL^{-1} toluene solution of each material on top of a nanocrystalline TiO_2 film, followed by electrolyte deposition). Device configuration and energy levels of the components are also displayed in Fig. 4a,b.

In a typical DSSC, upon irradiation, photoexcited dye molecules inject electrons into the TiO_2 conduction band, which can be extracted as a photocurrent. The circuit is closed with a counter-electrode and a hole transport medium (electrolyte), which replaces the lost electron (or hole) on the dye molecule. In the approach shown in Fig. 4 a, the polymer acts as the sensitizer, *i.e.*, absorbs light and then injects electrons into the conduction band of TiO_2. The electrons are transported to the transparent bottom electrode, while the oxidized polymer is regenerated to the ground state by the redox mediator (I_3^-/I^-) in the electrolyte.

There have been some reports using conjugated polymers as a sensitizer, but the overall power conversion efficiencies were observed to be low. A more effective way to explore this approach is by using polymers containing carboxylic groups [56–59], which enable the formation of chemical bonds with the TiO_2 surface therefore improving the efficiency of the charge injection processes.

In this work, the use of only P3HT as sensitizer did not lead to significant improvements in photocurrent (Jsc) or photovoltage (Voc) and also resulted in a great loss of fill factor (FF). This is due to the fact that the polymer layer is only physically adsorbed onto the TiO_2 film, since P3HT does not have carboxylic groups to chemically attach to the TiO_2, as sensitizers usually do. The lack of a chemical bond prevents efficient charge transfer between these materials. Only the excitons formed near the interface can split effectively and contribute to current collection. Besides, recombination between electrons injected into the conduction band of TiO_2 and holes in P3HT may also occur, since these materials are in direct contact.

When P3HT-Au is used as sensitizer, Jsc and Voc are significantly increased and this is possibly related to the plasmon contribution of the AuNPs. There are a few different mechanisms which may be considered as candidates for the plasmonic contribution to the short circuit current in a TiO_2 based DSSC [40], such as enhancement of the optical absorption in the range of visible light and enhancement in charge separation due to the electric field.

The use of P3HT-C_{60} copolymer was also found to increase both Jsc and Voc. In another study [46], the addition of P3HT-C_{60} copolymers containing different concentrations of C_{60} to the TiO_2 film in a DSSC was carried out. The photocurrent and photovoltage were found to be dependent on the concentration of C_{60} in the copolymers and the sample with the highest C_{60} content was the one that gave rise to the highest photovoltage. The idea of incorporating C_{60} at the TiO_2/electrolyte interface is based on the fact that layers of C_{60} can form a barrier against electron transfer, as well as a diffusion barrier to the movement of anions toward the photoanode [60]. Thus, the incorporation of a polymer containing C_{60} in a DSSC is expected to accelerate charge separation and prevent charge recombination. In this work, the improvements observed using P3HT-C_{60} may be related to the increased light-harvesting ability of this material, as evidenced in the absorption spectra (Fig. 1a).

Interestingly, when P3HT-C_{60}-Au is used as sensitizer, both Jsc and Voc are further increased. We believe this is a result of two contributions: (i) the light absorption and exciton generation in the polymer that increase due to the plasmon effect induced by the presence of AuNPs; and (ii) the presence of C_{60} in this layer which minimizes recombination processes.

A further investigation was performed by incorporating the synthesized nanocomposites as co-sensitizers in DSSCs, in combination with the well known N719 dye. The device configuration, energy levels and *J*–*V* curves are shown in Fig. 5.

The use of conjugated polymers as co-sensitizers in combination with several dyes has been shown previously. In some cases, the polymer is used as both a second-sensitizer and as a hole transporter material [35,61,62]. Using this approach, it is often difficult to determine whether or not P3HT has a role as a second-sensitizer due to the overlap of its absorption band with that of primary dyes. However, a few advantages are expected when combining dye molecules with polymers, as suggested by Lee et al. [61]: (1) the dye anchored to the surface of TiO_2 can improve the wetting of the oxide surface by the hydrophobic polymer, thus leading to an

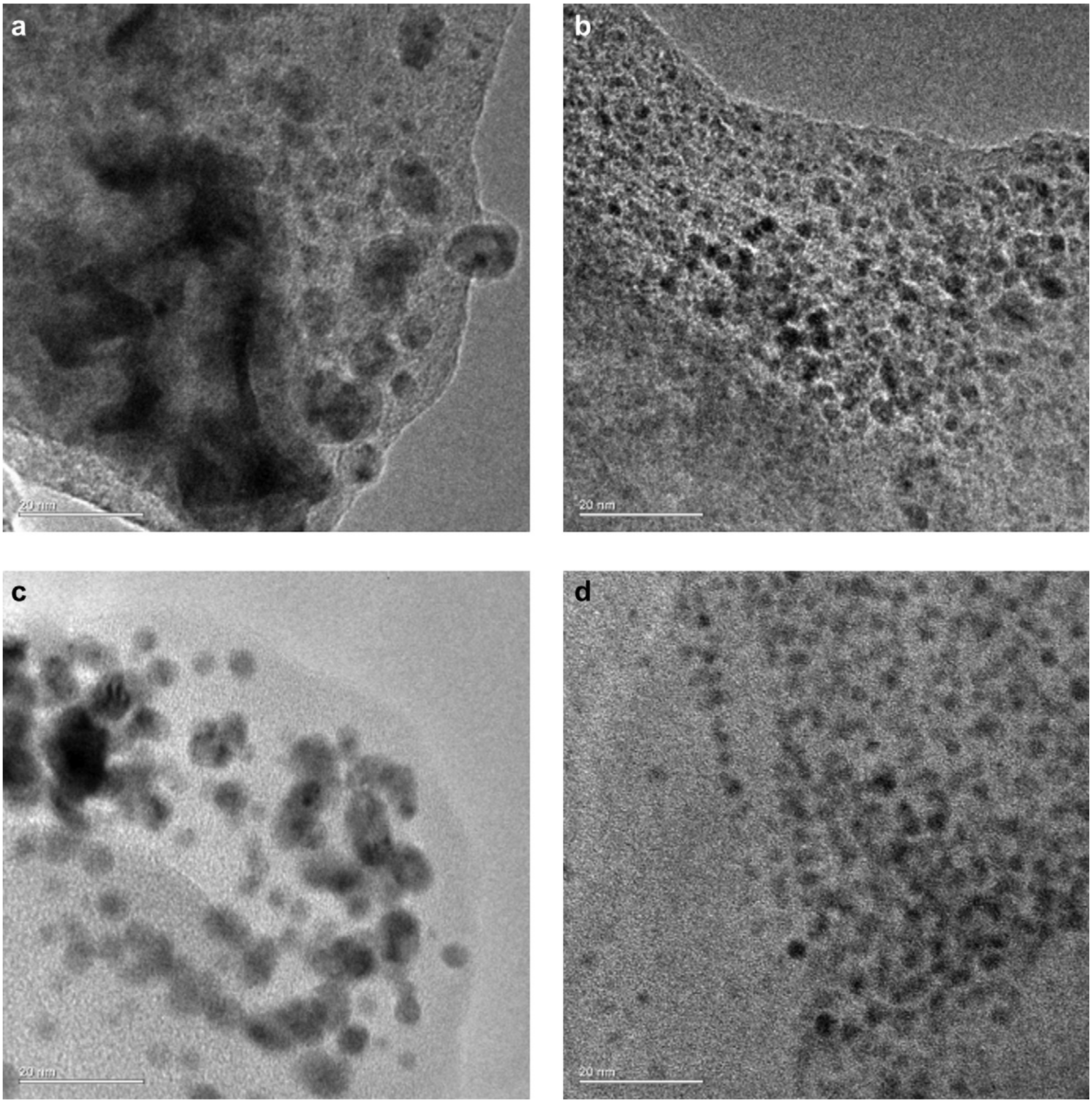

Fig. 3. HRTEM images of (a,b) P3HT-Au and (c,d) P3HT-C_{60}-Au nanocomposites, for two different regions of each sample. The scale bar indicates 20 nm in all images.

increase in the interfacial contact area for charge separation; (2) the dye placed between TiO_2 and the polymer can act as an electronic mediator to increase the efficiency of electron injection under the cascade band structures or it can separate the TiO_2 surface and P3HT properly, thus preventing direct contact and thereby suppressing the charge recombination between them; and (3) hole transfer from the dye to the polymer following excitation of the dye should happen, contributing to the increase of the absorbed light-to-current conversion efficiencies. Moon et al. [35] recently reported efficient energy transfer from the P3HT to a porphyrin dye. Their results corroborate the finding that P3HT can carry out dual functions in DSSCs, as a hole transport material and as a sensitizer. Kudo et al. [36] suggested that electron transfer from P3HT to TiO_2 through Ru-based dyes is thermodynamically allowed because of the appropriate gradient of energy levels. On the other hand, Zhang et al. [37] investigated DSSCs containing an organic indoline dye and P3HT and observed that P3HT contributed very little to the photocurrent and acted only as hole transport material.

In this work, the *J*–*V* characteristics shown in Fig. 5 reveal that incorporation of P3HT or P3HT-Au as co-sensitizers in combination with N719 decreased the overall device performance, due to the much lower photocurrent in these systems (see Table 2). From the dark *J*–*V* characteristics it can be seen that suppression of dark current is enhanced in the presence of P3HT and P3HT-Au. In the device containing only N719 dye, recombination is higher, as evidenced by the increased dark current. The separation of the ruthenium dye from the I_3^-/I^- redox couple in the electrolyte due to the presence of polymer chains (which creates a hydrophobic atmosphere, as shown by Schmidt–Mende et al. [63] for long alkyl chains) act as barriers for the recombination. Therefore, the lower charge extraction (photocurrent) observed in these systems may result from trapping of charges in the polymeric material and increased contact resistance (at the interface). The lower Voc observed is a consequence of less charge generation or flow through this device.

When P3HT-C_{60} copolymer is used in combination with N719, the device shows an increase in photocurrent, which was expected

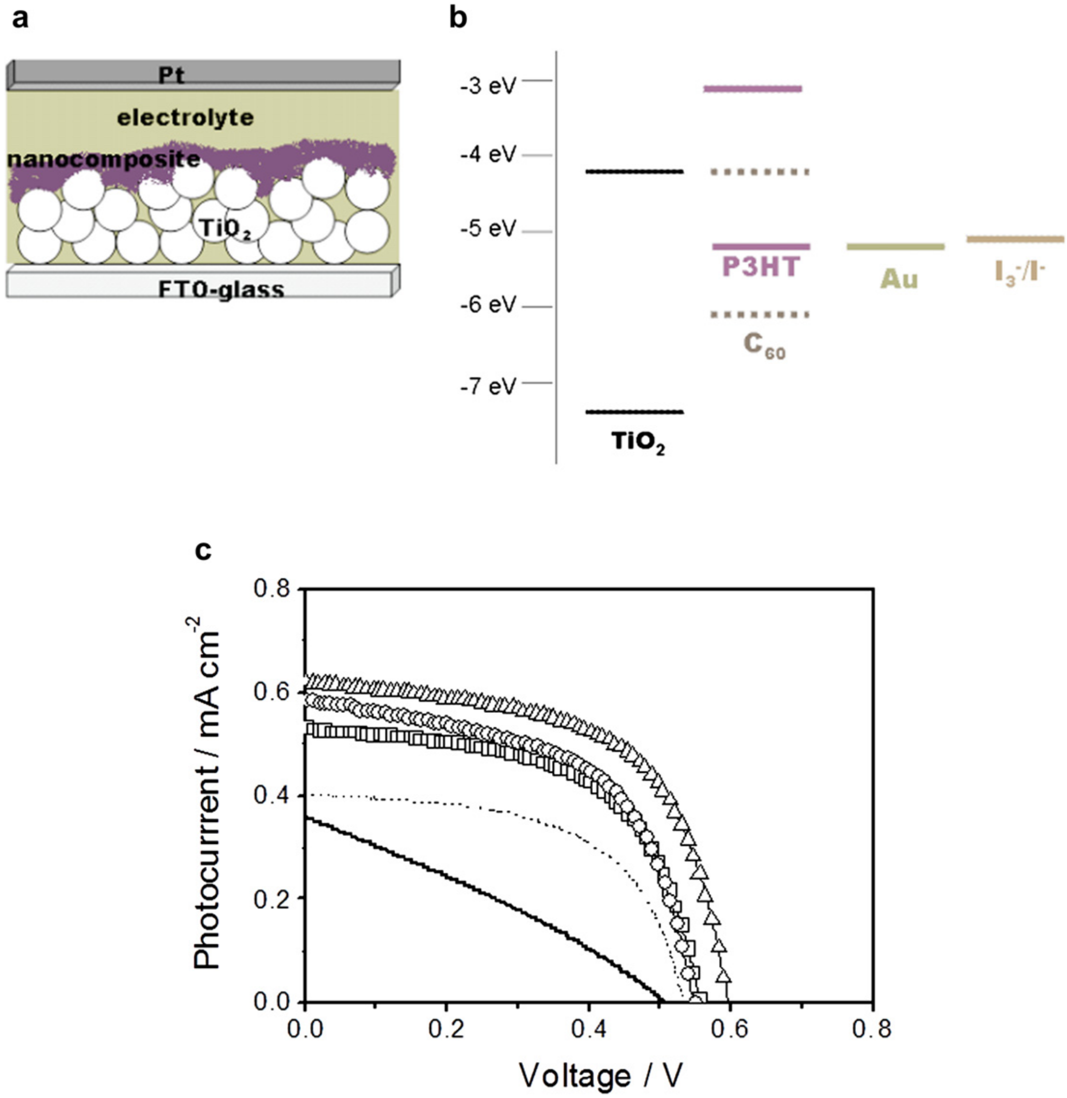

Fig. 4. Scheme of (a) device architecture, (b) energy levels of the components of the DSSC and (c) *J*–*V* characteristics of dye-sensitized solar cells assembled using (-) P3HT, (-□-) P3HT-Au, (-○-) P3HT-C_{60} and (-Δ-) P3HT-C_{60}-Au as sensitizers, or (——) without sensitizer (active area ∼0.15 cm^2; illumination of 100 mW cm^{-2}).

considering the broad absorption spectra of this material (Fig. 1a). Also, the presence of C_{60} was expected to minimize recombination: Kamat et al. [43] have reported that C_{60} clusters can act as an electron shuttle which effectively regenerates the sensitizer and at the same time minimizes direct interaction between the excited sensitizer and the redox couple in the electrolyte. This will reduce the rate of the back electron transfer from the TiO_2 conduction band to the I_3^- ions. This suppression should lead to an increase in Voc. We did not observe this effect. On the contrary, we observed a decrease in Voc. Lim et al. [64] showed that the energetic levels appear to be favorable for electron transfer from the conduction band of TiO_2 to I_3^- ions through C_{60} (see the LUMO position in Fig. 5b), facilitating the back electron transfer and thereby decreasing the Voc. These authors also reported that this effect was related to the distance of C_{60} in relation to TiO_2. In our case, back electron transfer to I_3^- ions via this pathway can explain the lower Voc observed for the devices containing nanocomposites as co-sensitizers, compared to the standard device assembled only with N719 dye. Indeed, recombination is higher in the presence of P3HT-C_{60} or P3HT-C_{60}-Au, as observed in the dark current characteristics in Fig. 5, related to the presence of C_{60} in these materials.

It is important to mention that for devices assembled with P3HT-C_{60} as co-sensitizer for N719, there is a balance between two opposite effects: (i) the increase in Jsc due to improved light-harvesting and (ii) the decrease in Voc due to enhanced recombination. This balance actually results in a small loss in the efficiency of the device, as can be seen in Table 2.

Interestingly, the use of the P3HT-C_{60}-Au nanocomposites again leads to a further increase in Jsc. This result reaffirms the synergistic effect that must exist between C_{60} and AuNPs. Due to the enhancement in Jsc, the efficiency of the device containing P3HT-C_{60}-Au as co-sensitizer was 5.9%, higher than the 5.2% obtained for the standard device containing only the N719 dye. In this case, the increase in Jsc related to enhanced light absorption and charge generation (see the much broader absorption profile of this material in Fig. 1 a) is more significant than the decrease observed in Voc (due to increased recombination), resulting in a more efficient device.

The exact role of each component of the ternary nanocomposite system in the DSSC is not yet clear. From the data collected, it is evident that the presence of both AuNPs and C_{60} can improve device performance. P3HT works as a matrix for the other two components and increases material solution processability.

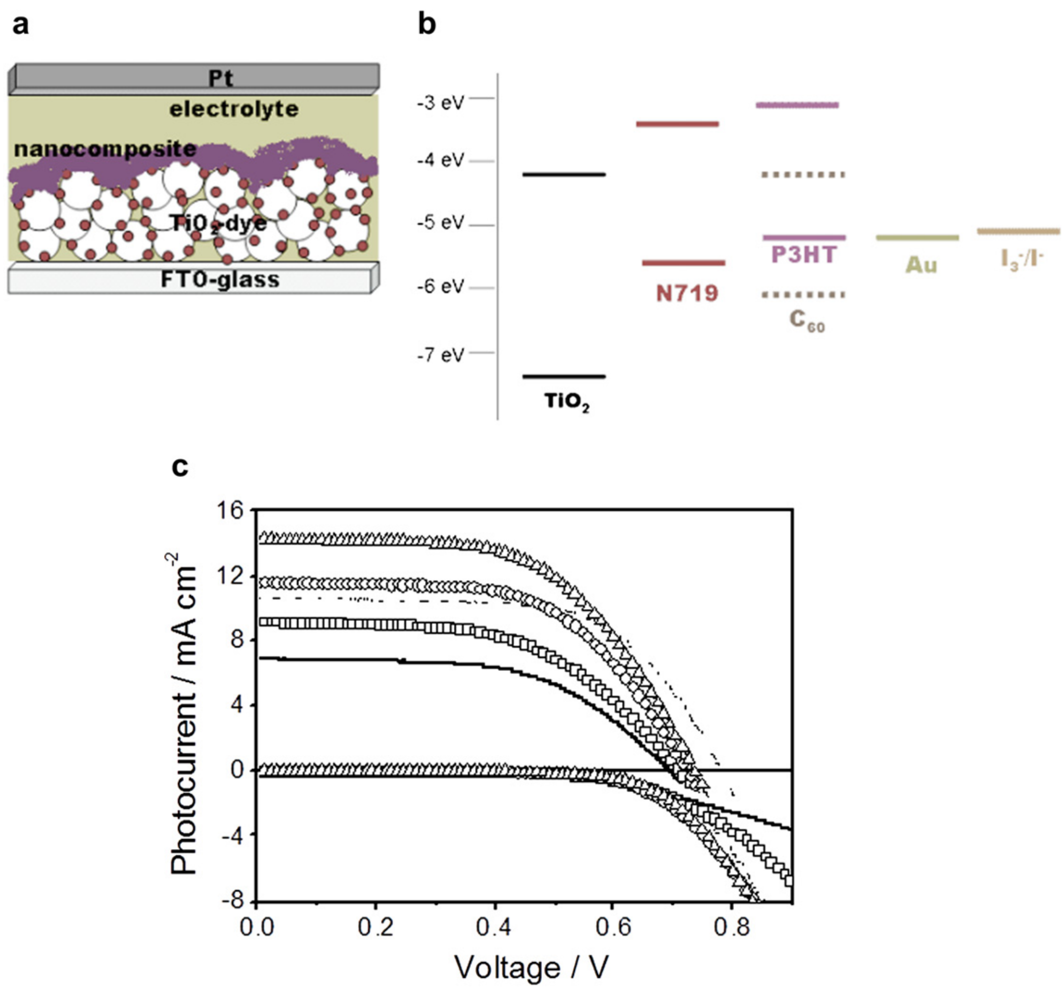

Fig. 5. Scheme of (a) device architecture, (b) energy levels of the components and (c) *J*–*V* characteristics in the dark and under irradiation (100 mW cm^{-2}) of dye-sensitized solar cells assembled using (…..) N719 as the only sensitizer or (▪) P3HT, (-□-) P3HT-Au, (-○-) P3HT-C_{60} and (-Δ-) P3HT-C_{60}-Au as co-sensitizers, together with N719 (active area ~ 0.15 cm^2).

Further optimization for the application of this type of nanocomposite in DSSCs must involve prevention of Voc loss, while increasing the photocurrent. It is also important to mention that it can be difficult to get reproducible data using this type of system, possibly due to a rather narrow pore size (less than 20 nm) for a complete infiltration of polymeric materials. Penetration of organic compounds into inorganic mesopores was also observed in typical solid-state DSSCs [65] and still remains one issue to be solved in this field. The optimization of the TiO_2 nanostructure using approaches such as tuning the pore size or employing nanotube arrays can be suitable alternatives to facilitate polymer infiltration and improve the performance of solid-state DSSCs.

Table 2
Parameters extracted from *J*–*V* curves for dye-sensitized solar cells assembled using the synthesized materials as sensitizer or co-sensitizer, under irradiation of 100 mW cm^{-2} (active area ~0.15 cm^2).

Sensitizer	Jsc/(mA cm^{-2})	Voc/(V)	FF/(%)	η/(%)
No sensitizer	0.40	0.53	61	0.13
P3HT	0.36	0.51	27	0.05
P3HT-Au	0.53	0.56	57	0.17
P3HT-C_{60}	0.59	0.55	55	0.18
P3HT-C_{60}Au	0.62	0.60	59	0.22
N719	10.64	0.78	63	5.20
N719 + P3HT	6.94	0.69	56	2.68
N719 + P3HT-Au	9.22	0.71	54	3.51
N719 + P3HT-C_{60}	11.57	0.72	59	4.90
N719 + P3HT-C_{60}Au	14.24	0.74	56	5.94

Usually, P3HT-C_{60}-based copolymers or composites are applied in OSC as an active layer. In this type of device, P3HT is responsible for the transport of holes, while C_{60} is responsible for the transport of electrons. The chemical bond between these materials is expected to minimize problems associated with phase separation and improve the charge transfer process (injection of electrons from the polymer into the fullerene). Many attempts to apply polymeric materials containing P3HT and C_{60} chemically bonded in OSC have been reported [7–9,17,66]. However, the efficiencies have so far been low, possibly due to poor morphologies and accelerated back reaction or fast rate of charge recombination, since electron donor and acceptor materials are linked or in close contact.

In this work, the incorporation of a 5 wt% of P3HT-C_{60} copolymer into a "standard" P3HT/PCBM bulk heterojunction slightly increased the photocurrent (see Supporting Information), possibly associated with a better control of morphology. This reinforces the belief that polymeric structures can be effectively designed to act as a compatibilizer in a "standard" OSC to improve device characteristics, as recently reported by Lee et al. [7]. The application of P3HT-

Au or P3HT-C_{60}-Au nanocomposites was not viable due to the frequent shorts observed, possibly associated with the large amount of gold in these materials. The materials were too conductive, with less photovoltaic properties and, therefore, the OSC lost performance. No benefits from the addition of AuNPs could be seen using this approach. In OSC, the use of small amounts of AuNPs are expected to enhance charge generation (due to the plasmon effect) and charge collection (due to the alignment of energy levels with PEDOT:PSS electrode).

An interesting alternative to be explored in the future is the application these nanocomposites as replacement for the liquid electrolyte in all-solid-state DSSCs.

4. Conclusions

In this work, new ternary-based nanocomposites consisting of P3HT, C_{60} and AuNPs were synthesized via a simple route: functionalized C_{60} was reacted with 3-hexylthiophene to form a copolymer, P3HT-C_{60}, which was then used to stabilize AuNPs. For comparison, a nanocomposite based on AuNPs stabilized with pristine P3HT was also prepared. The P3HT-C_{60}-Au nanocomposite was loaded with a larger amount of metal nanoparticles compared to the composite P3HT-Au, due to a different interaction between gold and thiophene units in these composites. These samples also have different optical characteristics. The application of these materials as sensitizers or co-sensitizers in dye-sensitized solar cells was found to be promising, and the largest photocurrent was obtained for the ternary component nanocomposite P3HT-C_{60}-Au. This was attributed to a synergistic effect between C_{60} and AuNPs, revealing the potential of exploring this type of material for energy conversion applications.

Acknowledgments

The authors thank the IBSA Project (fellowship Pró-África 490.490/2007-7), FAPESP (fellowship 2009/15428-0), CNPq and the National Research Foundation (NRF) for financial support; LME/LNNano/CNPEM for technical support during the HRTEM work; and Prof. Carol Collins for English revision.

Appendix A. Supplementary data

Supplementary data associated with this article can be found, in the online version, at doi:10.1016/j.jpowsour.2012.04.066.

References

[1] H. Imahori, K. Hagiwara, T. Akiyama, M. Aoki, S. Taniguchi, T. Okada, M. Shirakawa, Y. Sakata, Chem. Phys. Lett. 263 (1996) 545.
[2] N.S. Sariciftci, L. Smilowitz, A.J. Heeger, F. Wudl, Science 258 (1992) 1474.
[3] G. Yu, Y. Gao, J.C. Hummelen, F. Wudl, A.J. Heeger, Science 270 (1995) 1789.
[4] F. Padinger, R.S. Rittberger, N.S. Sariciftci, Adv. Funct. Mater. 13 (2003) 85.
[5] G. Li, V. Shrotriya, Y. Yao, J.S. Huang, Y. Yang, J. Mater. Chem. 17 (2007) 3126.
[6] H. Hoppe, N.S. Sariciftc, J. Mater. Res. 19 (2004) 1924.
[7] J.U. Lee, J.W. Jung, T. Emrick, T.P. Russell, W.H. Jo, J. Mater, Chem 20 (2010) 3287.
[8] B. de Boer, U. Stalmach, P.F. van Hutten, C. Melzer, V.V. Krasnikov, G. Hadziioannou, Polymer 42 (2001) 9097.
[9] K. Sivula, Z.T. Ball, N. Watanabe, J.M.J. Fréchet, Adv. Mater. 18 (2006) 206.
[10] H. Fang, S. Xiao, Y. Li, S. Xiao, H. Li, H. Liu, Z. Shi, D. Zhu, Synth. Met. 135-136 (2003) 837.
[11] M. Dante, C. Yang, B. Walker, F. Wudl, T.-Q. Nguyen, Adv. Mater. 22 (2010) 1–5.
[12] B.W. Boudouris, F. Molins, D.A. Blank, C.D. Frisbie, M.A. Hillmyer, Macromolecules 42 (2009) 4118.
[13] F. Richard, C. Brochon, N. Leclerc, D. Eckhardt, T. Heiser, G. Hadziiannou, Macromol. Rapid Commun. 29 (2008) 885.
[14] S. Barrau, T. Helser, F. Richard, C. Brochon, C. Ngov, K. van de Wetering, G. Hadziioannou, D.V. Anokhin, D.A. Ivanov, Macromolecules 41 (2008) 2701.
[15] Z.T. Ball, K. Sivula, J.M.J. Fréchet, Macromolecules 39 (2006) 70–72.
[16] A. Cravino, Polym. Int. 56 (2007) 943.
[17] A. Cravino, N.S. Sariciftci, J. Mater. Chem. 12 (2002) 1931.
[18] A. Cravino, G. Zerza, M. Maggini, S. Bucella, M. Scensson, M.R. Andersson, H. Neugebauer, N.S. Sariciftci, Chem. Commun. (2000) 2487.
[19] R. Morioka, K. Yasui, M. Ozawa, K. Odoi, H. Ichikawa, K. Fujita, J. Photopolym. Sci. Technol. 23 (2010) 313.
[20] F.-C. Chen, J.-L. Wu, C.-L. Lee, Y. Hong, C.-H. Kuo, M.H. Huang, Appl. Phys. Lett. 95 (2009) 013305.
[21] J.H. Lee, J.H. Park, J.S. Kim, D.Y. Lee, K. Cho, Org. Electron. 10 (2009) 413.
[22] S.-S. Kim, S.-I. Na, J. Jo, D.-Y. Kim, Y.-C. Nah, Appl. Phys. Lett. 93 (2008) 073307.
[23] A.J. Morfa, K.L. Rowlen, T.H. Reilly III, M.J. Romero, J. van de Lagemaat, Appl. Phys. Lett. 92 (2008) 013504.
[24] K. Kim, D.L. Carroll, Appl. Phys. Lett. 87 (2005) 203113.
[25] M. Park, B.D. Chin, J.-W. Yu, M.-S. Chun, S.-H. Han, J. Ind. Eng. Chem. 14 (2008) 382.
[26] K. Topp, H. Borchert, F. Johnen, A.V. Tunc, M. Knipper, E. von Hauff, J. Parisi, K. Al-Shamery, J. Phys. Chem. A 114 (2010) 3981.
[27] D.H. Wang, D.Y. Kim, K.W. Choi, J.H. Seo, S.H. Im, J.H. Park, O.O. Park, A.J. Heeger, Angew. Chem. Int. 50 (2011) 1–6.
[28] P.G. Nicholson, V. Ruiz, J.V. Macpherson, P.R. Unwin, Chem. Commun. 12 (2005) 1052.
[29] M.R.C. Hunt, S. Modesti, P. Rudolf, R.E. Palmer, Phys. Rev. B 51 (1995) 10039.
[30] L.H. Tjeng, R. Hesper, A.C.L. Heessels, A. Heers, H.T. Jonkman, G.A. Sawatzky, Solid State Commun. 103 (1997) 31.
[31] S.J. Chase, W.S. Bacsa, M.G. Mitch, L.J. Pilione, J.S. Lannin, Phys. Rev. B 46 (1992) 7873.
[32] G. L. C. Conturbia, Células solares baseadas em nanotubos de carbono modificado e nanopartículas de ouro. Master's Thesis, Universidade Estadual de Campinas, Campinas, 2009.
[33] J.N. de Freitas, A.F. Nogueira, in: F.L. de Souza, E.R. Leite (Eds.), Nanoenergy: Nanotechnolgy Applied for Energy Production, Springer-Verlag, 2012.
[34] X. Zheng, J. Zhang, L. Peng, X. Yang, W. Cao, J. Mater. Sci. 46 (2011) 5071.
[35] S.-J. Moon, E. Baranoff, S.M. Zakeeruddin, C.-Y. Yeh, E.W.-G. Diau, M. Grätzel, K. Sivula, Chem. Commun. 47 (2011) 8244.
[36] N. Kudo, S. Honda, Y. Shimazaki, H. Ohkita, S. Ito, H. Benten, Appl. Phys. Lett. 90 (2007) 183513.
[37] W. Zhang, R. Zhu, F. Li, Q. Wang, B. Liu, J. Phys. Chem. C 115 (2011) 7038.
[38] R. Zhu, C.-Y. Jiang, B. Liu, S. Ramakrishna, Adv. Mater. 21 (2009) 994.
[39] K.-J. Jiang, K. Manseki, Y.-H. Yu, N. Masaki, K. Suzuki, Y.-L. Song, S. Yanagida, Adv. Funct. Mater. 19 (2009) 2481.
[40] C. Hägglund, M. Zach, B. Kasemo, Appl. Phys. Lett. 92 (2008) 013113.
[41] S.D. Standridge, G.C. Schatz, J.T. Hupp, J. Am. Chem. Soc. 131 (2009) 8407.
[42] M. Grätzel, Nature 421 (2003) 586.
[43] P.V. Kamat, M. Haria, S. Hotchandani, J. Phys. Chem. B 108 (2004) 5166.
[44] M. Maggini, G. Scorrano, M. Prato, J. Am. Chem. Soc. 115 (1993) 9798.
[45] M.R. Andersson, D. Selse, M. Berggren, H. Jarvinen, T. Hjertberg, O. Inganas, O. ennerstrom, J.E. Oserholm, Macromolecules 27 (1994) 6503.
[46] M. A. Mamo, F. S. Freitas, J. N. de Freitas, W. A. L. van Otterlo, A. F. Nogueira, N. J. Coville, Poly(3-hexylthiophene) covalently linked to fullerene for use in hybrid solar cells, in press.
[47] M. A. Mamo, "Functionalization of carbonaceous materials for photovoltaic devices" PhD Thesis, University of the Witwatersrand, Johannesburg, 2010.
[48] L. Zhai, R.D. McCullough, J. Mater. Chem. 14 (2004) 141.
[49] U. Stalmach, B. de Boer, C. Videlot, P.F. van Hutten, G. Hadziioannou, J. Am. Chem. Soc. 122 (2000) 5465.
[50] S. Hotta, S.D.D.V. Rughooputh, A.J. Heeger, F. Wudl, Macromolecules 20 (1987) 212.
[51] J.H. Youk, J. Locklin, C. Xia, M. Park, R. Advincula, Langmuir 17 (2001) 4681.
[52] R.D. McCullough, S.P. Tristam-Nagle, R.D. Lowe, M. Jayaraman, Am. Chem. Soc. 115 (1993) 4910.
[53] T. Erb, U. Zhokhavets, G. Gobsch, S. Raleva, B. Stühn, P. Schilinsky, C. Waldauf, C.J. Brabec, Adv. Funct. Mater. 15 (2005) 1193.
[54] S. Hugger, R. Thomann, T. Heinzel, T. Thurn-Albrecht, Colloid Polym. Sci. 282 (2004) 932.
[55] H.P. Klug, L.E. Alexander, X-Ray Diffraction Procedures, Wiley, Nova Iorque, 1954.
[56] J.C. Fatuch, M.A. Soto-Oviedo, C.O. Avellaneda, M.F. Franco, W. Romão, M.-A. De Paoli, A.F. Nogueira, Synth. Met. 159 (2009) 2348.
[57] S. Yanagida, G.K.R. Senadeera, K. Nakamura, T. Kitamura, Y. Wada, J. Photochem. Photobiol. A 166 (2004) 75.
[58] R.H. Lohwasser, J. Bandara, M. Thelakkat, J. Mater. Chem. 19 (2009) 4126.
[59] G.K.R. Senadeera, T. Kitamura, Y. Wada, S. Yanagida, Sol. Energy Mater. Sol. Cells 88 (2005) 315.
[60] S.-Y. Oh, S.-H. Han, Synth. Met. 121 (2001) 1369.
[61] H.J. Lee, H.C. Leventis, S.A. Haque, T. Torres, M. Gratzel, M.K. Nazeeruddin, J. Power Sources 196 (2011) 596.
[62] Y. Saito, T. Azechi, T. Kitamura, Y. Hasegawa, Y. Wada, S. Yanagida, Coord. Chem. Rev. 248 (2004) 1469.
[63] L. Schmidt-Mende, J.E. Kroeze, J.R. Durrant, M.K. Nazeeruddin, M. Grätzel, Nano Lett. 5 (2005) 1315.
[64] M.K. Lim, S.-R. Jang, R. Vittal, J. Lee, K.-J. Kim, J. Photochem. Photobiol. A 190 (2007) 128.
[65] L. Schmidt-Mende, M. Grätzel, Thin Solid Films 500 (2006) 296.
[66] A. Cravino, G. Zerza, M. Maggini, S. Bucella, M. Svensson, M.R. Andersson, H. Neugebauer, C.J. Brabec, N.S. Sariciftci, Monatsh. fur Chem. 134 (2003) 519–527.